Journal of Biomedical Optics

BiomedicalOptics.SPIEDigitalLibrary.org

No-core fiber-based highly sensitive optical fiber pH sensor

Vanita Bhardwaj
Akhilesh Kumar Pathak
Vinod Kumar Singh

SPIE.

Vanita Bhardwaj, Akhilesh Kumar Pathak, Vinod Kumar Singh, "No-core fiber-based highly sensitive optical fiber pH sensor," *J. Biomed. Opt.* **22**(5), 057001 (2017), doi: 10.1117/1.JBO.22.5.057001.

No-core fiber-based highly sensitive optical fiber pH sensor

Vanita Bhardwaj,* Akhilesh Kumar Pathak, and Vinod Kumar Singh
Indian Institute of Technology (Indian School of Mines), Department of Applied Physics, Dhanbad, Jharkhand, India

Abstract. The present work describes the fabrication and characterization of an optical fiber pH sensor using a sol–gel technique. The sensing head configuration is incorporated using a short section of no-core fiber, coated with tetraethyl orthosilicate and spliced at the end of a single mode fiber with a bulge. Different types of indicators (bromophenol blue, cresol red, and chlorophenol red) were used to achieve a wide pH range from 2 to 13. High sensitivities of the fabricated device were found to be 1.02 and −0.93 nm/pH for acidic and alkaline solutions, respectively. From the characterization results, it was noted that there is an impact of ionic strength and an effect of the temperature of liquid on the response characteristic, which is an advantage of the existing device over the other pH sensors. The fabricated sensor exhibited good reflection spectrum, indicating a blueshift in resonance wavelength for alkaline solutions and a redshift for acidic solutions. [DOI: 10.1117/1.JBO.22.5.057001]

Keywords: organic dyes; pH sensor; sol–gel; no-core fiber.

Paper 170023R received Jan. 19, 2017; accepted for publication Apr. 17, 2017; published online May 5, 2017.

1 Introduction

Optical fiber-based pH sensors have become one of the hot topics in the field of research due to their numerous advantages such as being light weight, small in size, and highly sensitive and having fast response, immunity to electromagnetic radiations, radio frequency interference, good repeatability, and stability over conventional sensors. Indeed, the accuracy level in measuring pH values for liquids is the key focus in the fabrication of optical-based pH sensors. These sensors have a wide range of application in many scientific areas such as clinical, health monitoring, biotechnology, and process control in industry. Thus, various methods have been developed to fabricate pH sensors[1–3] using optical fibers.

In the last decade, numerous studies have been conducted to study the variations of optical properties for pH indicators. Sensors depend on these methods to detect pH value of liquids by variations in absorption due to changes in the color of indicators. These devices have low sensitivity over a limited pH range. In addition, these sensors were unable to measure OH^- ions. Optical fiber-based pH sensors are usually based on the reflection principle and evanescent-wave, and these sensors can be easily used in medical science. Kasik et al. presented a measurement of pH in microscopic biological samples,[4] Grant et al. presented measurements of fiber optic and electrochemical sensors to monitor brain tissue pH,[5] and Peterson et al. showed an optical fiber pH probe for physiological use.[6] Various approaches have been applied to increase the sensitivity of fiber-optic pH sensing probes. In this regards, Ondrej et al. fabricated a tapered optical fiber sensor for detection of pH in microscopic volumes,[7] Rickelt et al. proposed a method for shaping the measuring tip using an etching method,[8] and Gupta and Sharma fabricated U-shaped fiber-optic pH probes.[9]

The pH detecting film prepared using sensitive dyes also plays an important role in enhancing the sensitivity of devices. The indicator-based pH sensors have also been reported earlier.[10,11] Owing to its cost effective and simple procedure, the sol–gel technique was used for immobilization of pH-sensitive dyes on the fiber surface.[12–16] Sol–gel technology has many advantages over other film deposition methods. In aggressive environments, the sol–gel film is more resistant, inert, and tough compared to polymer films. The pH-sensing fiber probe is prepared by depositing a pH-sensitive dye on the surface of the sensing length using sol–gel technology. These organic dyes are typically supported by the precursor solution of tetraethyl orthosilicate (TEOS). The pH-sensing film was deposited on fiber probe using a dip-coating mechanism, and the pH-sensing solution for the coating process was prepared by mixing different pH-sensitive dyes including TEOS as precursor materials. Numerous efforts have been directed toward the development of pH sensors to perform *in vivo* analysis and *in situ* monitoring. Tapered optical fiber probes also offer various advantages over other ones, such as small size and enhanced sensitivity, which could be used in pH sensors.

The present work describes the fabrication of an optical fiber-based pH sensor using a configuration for pH sensing that consists of a no-core fiber (NCF) with a bulge at the end of a single mode fiber (SMF); it extends the multipoint sensing compared to other conventional devices for pH sensing to the best of our knowledge. The pH-sensitive coating was prepared by mixing different pH-sensitive dyes with TEOS as a precursor and depositing it on the fiber probe by dip coating. The sensor response was observed from the shift in resonance wavelength dip of the reflection spectra due to the variation of pH levels from acid to alkaline solutions. In addition, the impact of ionic strength, refractive index detection, and effect of temperature of the

*Address all correspondence to: Vanita Bhardwaj, E-mail: vanitabhardwaj@ap.ism.ac.in

1083-3668/2017/$25.00 © 2017 SPIE

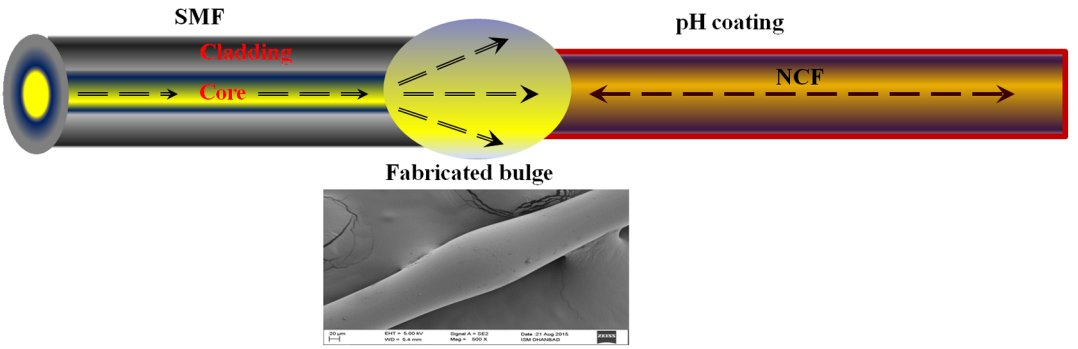

Fig. 1 (a) Schematic diagram of the optical fiber pH sensor with SEM image of the bulge.

liquid, which are additional advantages of the present device over other pH sensors, have been reported.

2 Experiment

2.1 *Fabrication of Fiber Probe*

The optical fiber probe was fabricated using the repeated arc function of a fusion splicing machine. The SMF has a core/cladding diameter of 8.5/125 μm, and the diameter of the NCF used in the present work is 96 μm. The NCF was used instead of multimode fiber (MMF) because no-cladding exhibits more sensitive response to the environment than traditional fibers. In the present work, we use NCF instead of MMF with a simple splicing condition to fabricate sensor configurations. The air cladding in NCF helps to achieve higher sensitivity. The output spectrum was recorded with variations of surrounding environment, and the shifts in wavelength were observed due to the direct contact of NCF with sensing component. The eigenmodes can be easily excited when the light propagates through NCF from an SMF. Many experimental results proved that the NCF helps to enhance the optical fiber sensor because of the strong interaction between the evanescent wave and the surrounding environment. In addition, in NCF, the effective refractive index of modes are strongly affected by the surrounding environment.

As the first step of fabrication, SMF was first striped and cleaved. A small section of NCF was then spliced with SMF using the repeated arc function of a fusion splicer (Sumitomo Electric, type 39) set to manual mode. The primary splicer parameters used for the fabrication of the device were an overlap of 80 μm, a splicing fusion time of 0.62 s, and an arc discharge repeated up to 54 times. The repeated arc function of fusion splicer was used to fabricate bulge at the splice joint of both fibers. After cooling, a small section of the NCF fiber was then carefully cut in such a way that 1.5 cm length of NCF was left, which acted as the sensing probe. The schematic representation and scanning electron microscope (SEM) image of the bulge-shaped fiber structure is shown in Fig. 1.

Table 1 pH transition range of indicator dyes used in fabricating sensor.

Indicator dyes	pH transition ranges	Mass/volume (purity concentration)
Bromophenol blue	4.5 to 7.5	180 mg/ml
Cresol red	6.5 to 11	130 mg/ml
Chlorophenol red	8.5 to 13	130 mg/ml

2.2 *Preparation of pH-Sensing Coating*

In our experiment, TEOS was used as the precursor for the sol–gel preparation, and cresol red, chlorophenol red, and bromophenol blue were used as pH indicators, whose pH transition ranges are listed in Table 1.

The dyes exhibit intermediate colors at different pH values, which are evident from Table 1. But this range may shift depending on the concentration of the indicators and the temperature variation. Also, the pH measurement of liquid depends on the pK_a (dissociation constant) value of the dye. The dissociation constant value of the dye extends the pH measurement range. Consequently, it has been proposed that the pH measurement range can be extended using indicators with two or three pK_a values. Accordingly, we enhanced the dynamic pH measurement range of sensor by increasing the concentration of bromophenol blue. Anhydrous ethanol was used as a solvent because TEOS is insoluble in water. Initially, 100-ml TEOS was mixed with 100-ml anhydrous ethanol and 5-ml diluted HCL. The 2-ml deionized water with 46-mg cresol red, 42-mg chlorophenol red, and 82-mg bromophenol blue indicator dyes were then mixed by stirring the solution for 8 h at room temperature. Thus, pH measuring range can be tailored using an appropriate amount of different indicator dyes.

The violent catalyzation of hydrolysis is a common problem for pH sensing in an alkaline environment. To overcome this problem, diluted hydrochloric acid was mixed in the solution because the diluted HCl acts as a catalyst in alkaline environments to achieve good pH sensitivity.

2.3 *pH Coating on Fiber Probe*

The fabricated fiber probe was cleaned with acetone, dried, and then dipped in 30% concentrated HNO_3 to activate the OH group. These OH groups will help to bond the silica molecules on the fiber core surface and stick a thin film on the surface. The fiber probe was further cleaned with acetone. The uncladded fiber was then dipped and coated with the prepared long range pH-sensitive solution. The pulling speed of dip coater was 10 cm/min. After coating, the fiber was dried in oven at temperature at 60°C for 12 h. Further, the excess and unbounded dyes were removed by dipping the sample in water.

3 Sensing Principle

The work focuses on the fabrication of a refractive index-based pH sensor. Essentially, in principle, introduction of the fiber

probe into the analyte leads the variations in the refractive index of the cladding and is attributed to the penetration of analyte through the cladding. The theory can explain on the ground that when the guided light from lead-in SMF approaches the bulge region, the fundamental modes diverge and a fraction of it gets coupled into the NCF. These lead to the excitement of multiple modes propagated into the NCF then get reflected back at the end of the fiber before coupling into the bulge region. Further, two parts of light will reflect at the bulge and be recoupled into the core of lead-in SMF at the misalignment-splice joint, resulting in Michelson interference (MI) in the core of the SMF. Thus, an MI-based sensor was achieved.

According to MI, the fringe contrast in the interference pattern depends strongly on the ratio of lights coupled into the core and cladding modes in the NCF and their transmission loss. The relative phase displacement of the interfering two modes can be described as

$$2\pi[n_{\text{eff}}^{\text{co},}(\lambda) - n_{\text{eff}}^{\text{clad},j}(\lambda, n_{\text{ext}})]\frac{L}{\lambda} = (2k+1), \quad (1)$$

where $n_{\text{eff}}^{\text{co}}$ is the effective index of the core mode, $n_{\text{eff}}^{\text{clad},j}$ is the effective index of the j'th order cladding mode, n_{ext} is the RI of the surrounding medium, L is the length of the inserted fiber, λ is the wavelength of the transmission dip, and k is an integer.[17,18] The variation of pH value can be measured by observing the change in indicators on the surface of the fiber probe from protonated form to deprotonated form, and at the same time one can observe the variation of the indicator from negative to more negative. This leads to a change in electron density with the increment of the refractive index cladding. Thus, when the proposed device is exposed to liquids of different pH values having different RI, the effective RI of cladding modes will be influenced, but the fundamental mode is unaffected. The effective index of the cladding mode depends on the external RI; thus, the resonance wavelength will shift toward the shorter or longer wavelength if the external RI is varied.

4 Characterization of Fiber Probe

The experimental setup for the pH-sensing application is incorporated in Fig. 2. Light from a broadband source (BBS) with an operating wavelength of 1400 to 2000 nm is launched into the fabricated fiber with the help of the coupler. The fabricated fiber was mounted perpendicular to the bottom surface of the beaker to avoid the bending loss, and the beaker was filled with deionized water. The pH value of the liquid was varied by adding HCl and HNO_3. To calibrate the device and to detect the pH value, a pH electrode was introduced into the glass beaker. The other end of circulator was connected with an optical spectrum analyzer to analyze the optical spectrum.

Prior to the sol–gel coating and pH response test, the fabricated sensor was immersed in the mixed solution of sodium chloride (NaCl) and deionized water with different concentrations. The optical output is measured for the different RI of the solutions. The experimental setup is already described in Fig. 2, excluding the pH meter. The measured wavelength shifts of the interferometer as a function of refractive indices are shown in Fig. 3.

Before sol–gel coating, the immersion of the fabricated device into the RI solution shows the wavelength dip shift toward shorter wavelength with a sensitivity −329.36 nm/RIU. Table 2 shows some published results for comparison.

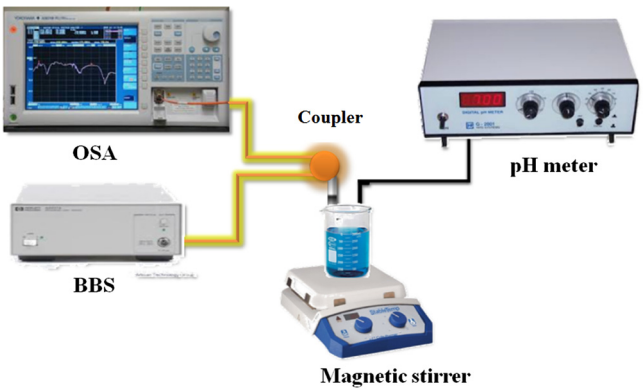

Fig. 2 Schematic of the experimental setup used to study the pH sensor.

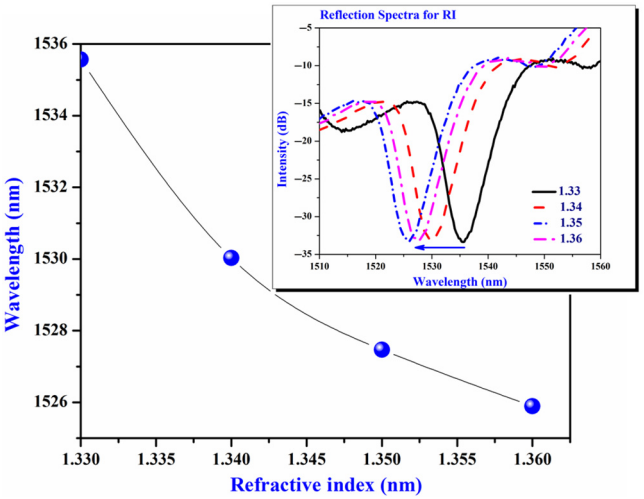

Fig. 3 Wavelength shift along with RI of NaCl solution before sol–gel coating and reflection spectra.

Table 2 Result comparison of fabricated device with other previous device.

S. no.	Type of sensor reference year sensitivity
1.	Multipoint fiber optic RI sensor[19] 2016 148.60 nm/RIU
2.	Connector off-set optical fiber sensor[20] 2016 197.33 nm/RIU
3.	Up tapered joint based RI[21] 2015 252.0 nm/RIU
4.	Core-off set SMF[22] 2015 78.7 nm/RIU based

5 Results and Discussions

To characterize the interference, light from the BBS launched into the fabricated sensor and output spectrum was recorded by optical spectrum analyzer (OSA). The reflectance spectra for prepared sol–gel at different temperatures after the sol–gel coating and without coating were recorded by an OSA for comparison. The fabricated device was used to obtain the reflection spectra of acidic and alkaline solutions ranging from 1510 to 1555 nm. After coating, a blueshift was observed in the interference spectrum that is attributed to the high RI of the pH-sensitive

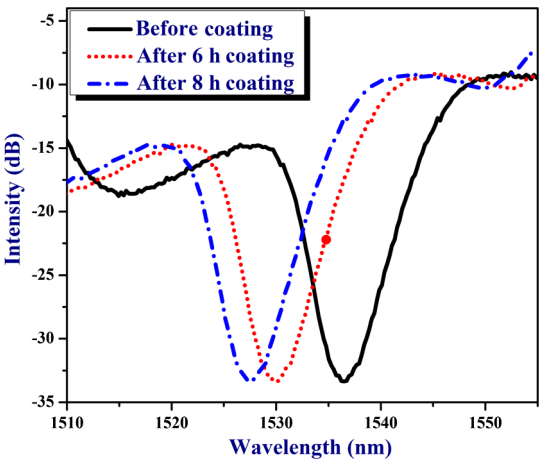

Fig. 4 Wavelength shift along with before and after sol–gel coating.

coating on the fiber probe. As shown in Fig. 4, the fabrication shows a reflection dip at 1536.23 nm, resulting in destructive interference. The wavelength dip at 1536.23 nm shifts to 1529.94 and 1527.52 nm after coating the fiber with sol–gel prepared at 6 h heating, coating and 8 h heating coating respectively at 50°C temperatures. This indicates that the sol–gel coating induced changes of the effective index.

The fabricated device was tested with acidic and alkaline solutions. The pH of the solutions was verified using a pH-meter with accuracy, ±0.01 pH units, and was adjusted when necessary by adding a few drops of HCl or HNO_3. Figure 5 shows the spectral response of a device for acidic and alkaline solutions. It can be observed that the wavelength dip of the optical spectrum shifts toward the shorter wavelength direction with an increase in ambient pH for alkaline solutions. Consequently, for acidic solutions, the wavelength dip of the optical spectrum shifts toward longer wavelengths with increasing pH values. The

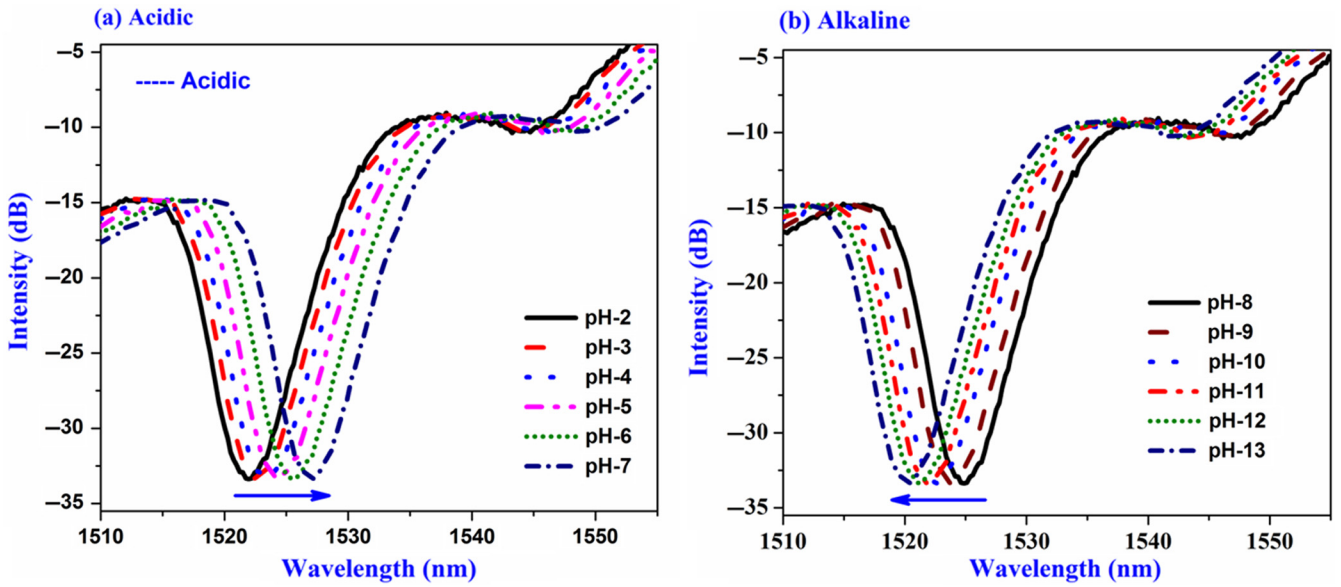

Fig. 5 The response of the fabricated device for (a) acidic solutions and (b) alkaline solutions.

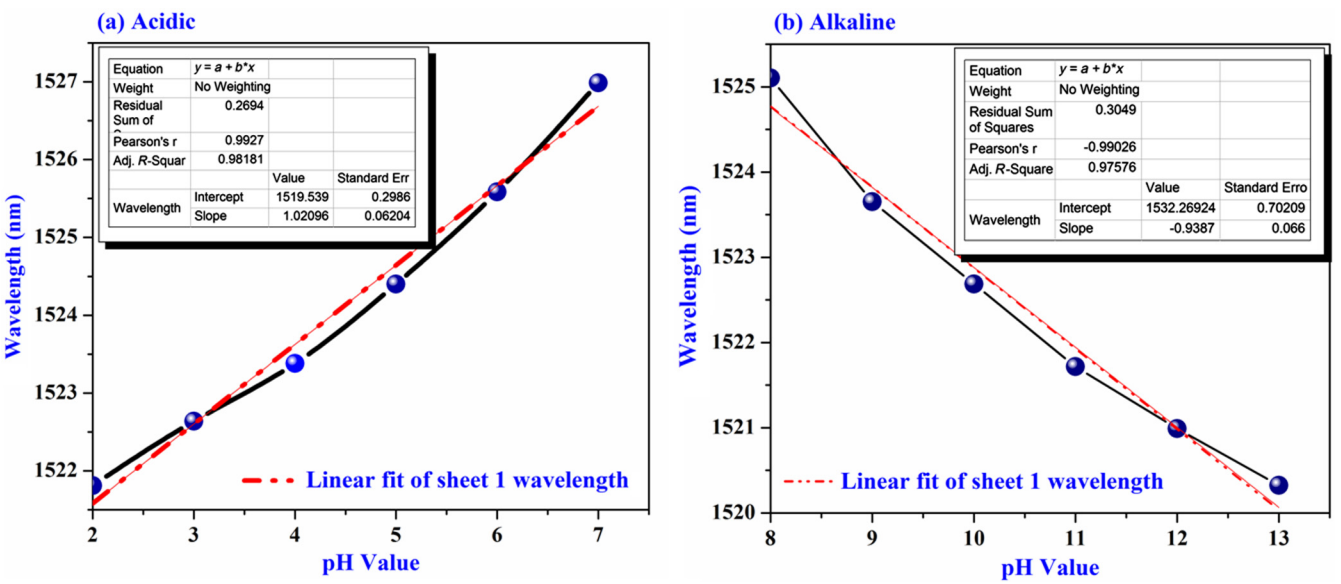

Fig. 6 Relationship between pH value and wavelength: (a) acidic solutions and (b) alkaline solutions.

Table 3 Result comparison of fabricated device with other previous device.

S. no.	Type of sensor reference year sensitivity
1.	Thin polymeric coating based[23] 2011 0.027 nm/pH
2.	Nanostructure cavity based[24] 2009 0.051 nm/pH
3.	Polyvinyl alcohol/polyacrylic[25] 2015 0.9 nm/pH acid based

modulation that took place in the ionization state of sol–gel by pH variations is responsible for this process. The modulation of ionization state of sol–gel-coating induces a change in its RI. The fabricated device performs in both low and high pH ranges with negligible effects from environmental temperature.

As can be seen from Fig. 6, resonance wavelength and pH are close to a linear relationship. The resonance wavelength 1527.52 nm was chosen as an indicator to demonstrate the ability of device pH response. The sensitivity of the device was obtained by calculating the slope of the curve.

The sensitivities of the fabricated device are 1.02 and −0.93 nm/pH for acid and alkaline solutions, respectively. Table 3 displays the different sensitivity data of reported sensor devices.

The experiment was repeated by taking the same fiber probe for a different coating heating time from 8 to 6 h. This alteration of coating heating time for coating affects the linearity of the device response. Figures 7 and 8 show the sensor response and relationship between pH value with wavelength for both acidic and alkaline solutions with sol get coating prepared after 6 h coating.

Polycondensation reaction is slow at room temperature. Consequently, the hydrolysis reaction is fast at room temperature. At a higher temperature, a catalyst can accelerate the hydrolysis and polycondensation reaction, which influences

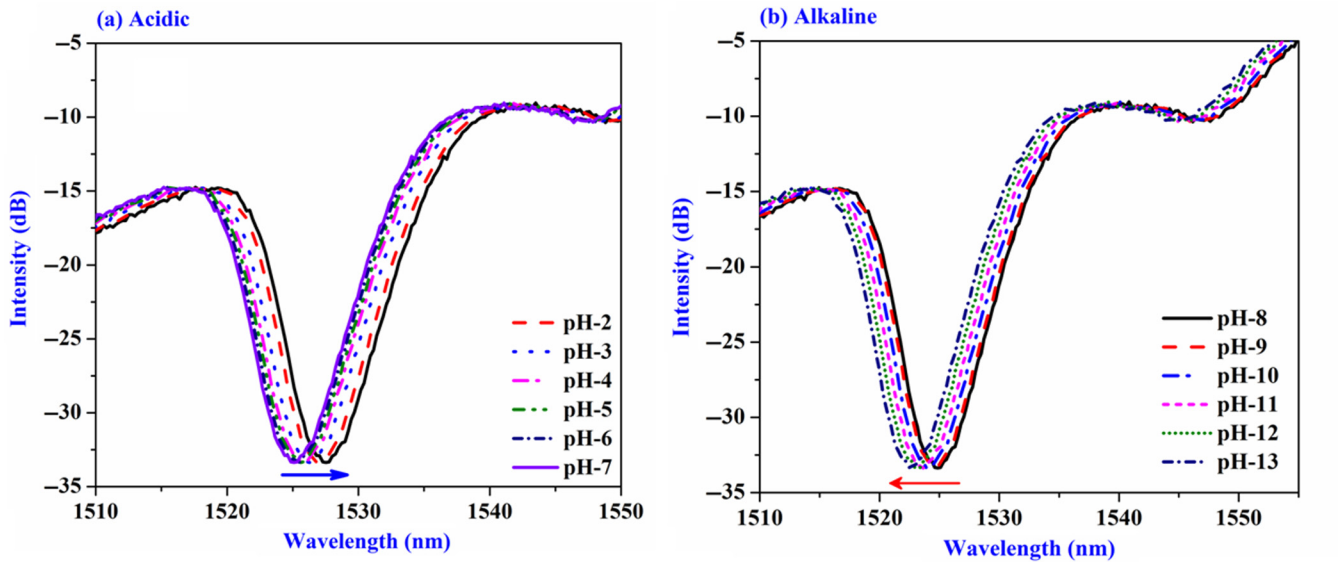

Fig. 7 The response of the fabricated device for (a) acidic solutions and (b) alkaline solutions.

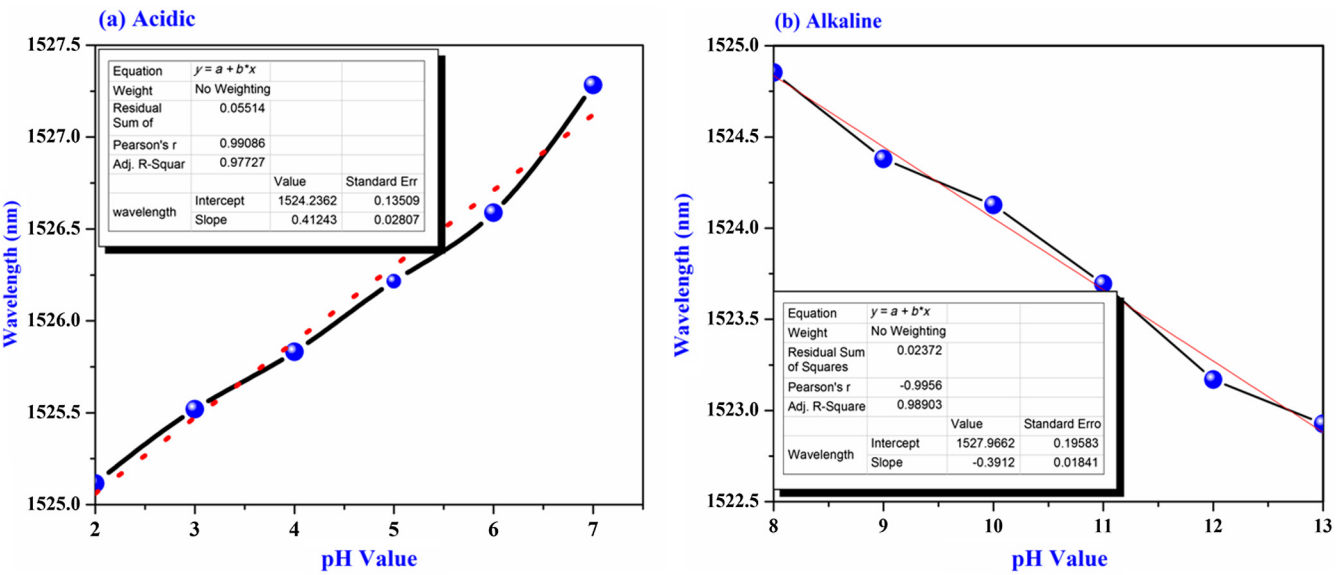

Fig. 8 Relationship between pH value and wavelength: (a) acidic solutions and (b) alkaline solutions.

the final form of pH-coating material and pH sensitivity. Various catalysts determine different chemical reactions, which generate different structures of pH-sensitive coating causing different pH sensitivities. Higher catalyst concentrations lead to shorter sol–gel forms, which is not conductive to the sensor repeatability coating. Therefore, a concentration of catalyst and variation of temperature during reaction is most important when the experiment is carried out.

The fabricated device was further investigated for its repeatability and stability. The stability and repeatability of the device are shown in Fig. 9. The wavelength shift of the device under different pH values in both ascending and descending orders is shown in Fig. 9(a). When the pH value decreases from 13 to 8, the wavelength dip shifts back to longer wavelengths. It is noted that the wavelength dip shifts from 1520.46 to 1525.114 nm with a sensitivity of 0.93 nm/pH. The stability results were obtained by testing the sensor under three constant pH values of 8, 10, and 12. The experimental result shows that the sensor has a good stability with negligible variation (0.0015 nm/pH).

To prove the reproducibility of the construction process to detect pH and compare the sensitivity of first device, two more devices with similar configurations were fabricated with the same pH-coating material because device performance depends on various factors such as electric arc discharge of the fusion splicer to fabricate up-taper region, splicing loss, fabrication of pH-coating matrix, amount of pH indicators used, coating thickness, swell and shrink of matrix with variation of pH values due to the variations in RI of matrix, activation of OH groups, catalyst, and environmental effect. These factors generate different structures of pH-sensitive coatings. Also, the measurement of the experiment depends on the measuring equipment (measuring instrument, calibration, etc.), people (operators, training, care, and education skill), process (test method and specification), sample materials, sample preparations, and environment. The authors tried their best to keep all these parameters

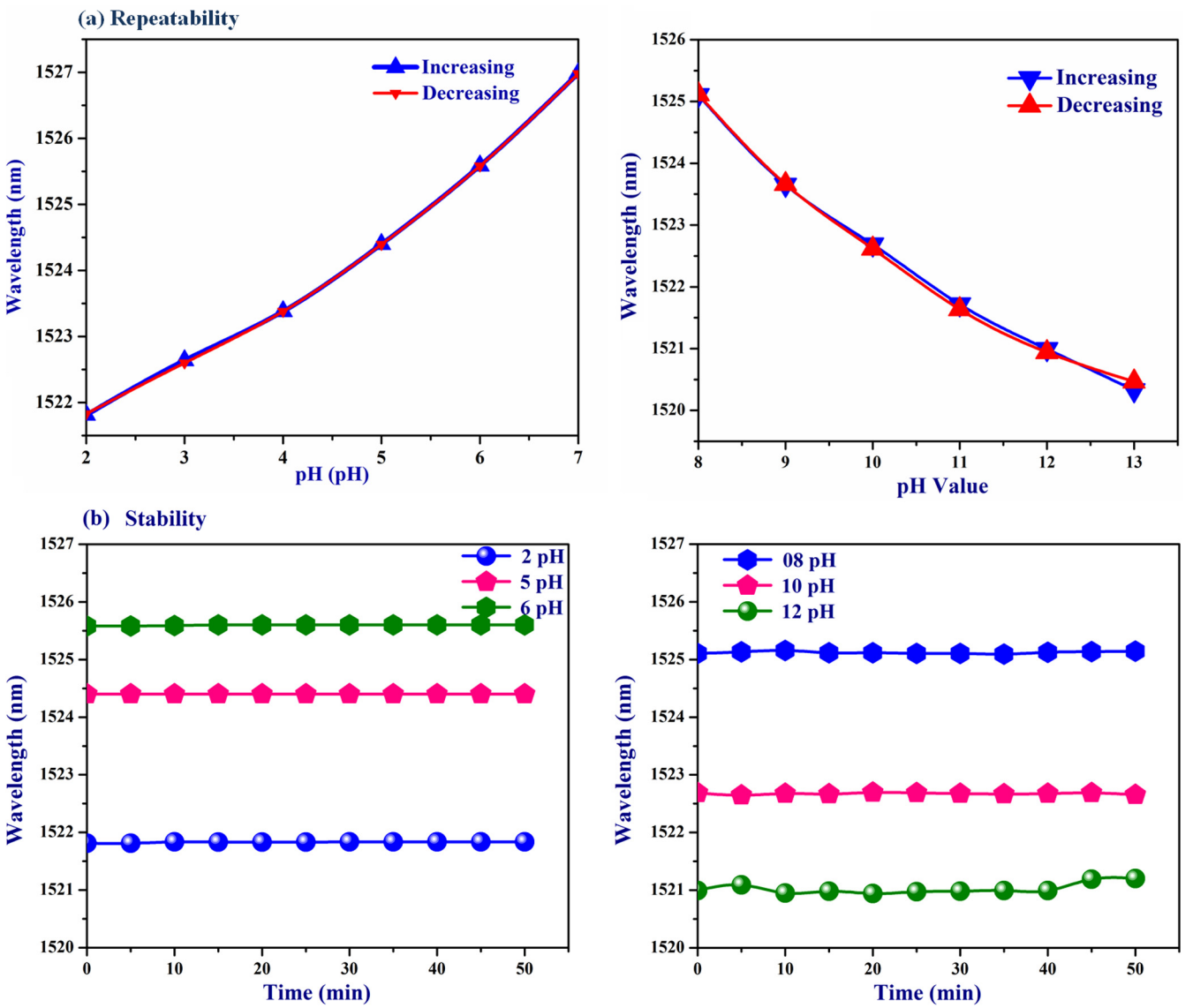

Fig. 9 (a) Repeatability of fabricated probe for ph sensing applications and (b) stability of fabricated probe for pH-sensing applications.

the same to enable the observations within same range, and they got the same result with negligible variations.

6 Analysis of the Influence of Other Technological Parameters

6.1 *Calibration Curve*

To examine the repeatability/reproducibility of the fabricated device, the experiment was successively carried out several times for 7 and 15 days at a constant temperature and a range of pH from 7 to 13. The device was properly dried before using it each time. Small fluctuations in reproducibility and sensitivity were observed each time with small variations in sensitivity. Figure 10 depicts the wavelength as a function of the range of pH.

6.2 *Impact of Ionic Strength and Temperature of Liquid*

The impact of ionic strength of the sensing fiber was verified by varying the molar value from 0 to 1 M. Figure 11 shows the dependence of the sensing fiber on the ionic strength of solutions. The solution was prepared using 0.04-M sodium acetate, 0.04-M sodium dihydrogen phosphate, and 0.04-M boric acid in deionized water for ionic strength measurement. Different solutions with variations of ionic strengths 0, 0.5, and 1 M were prepared by adding different amounts of sodium sulfate in the buffer solution.

It is observed from Fig. 11 that the wavelength shift increases with molar concentration. The curve of wavelength shift becomes steeper with the increase of ionic strength. This is due to the electrostatic interaction that screens the activity of the H^+ and OH^- ions since the pH sensors are sensitive to the protonated and deprotonated forms of indicator dyes that depend on the concentration of H^+ and OH^- ions, rather than the measured activities. The fabricated device shows less swelling behavior under low ionic concentrations. Thus, our device is suitable for 1 M concentration strength because a higher ionic strength makes it very difficult for the device to maintain the volume of the pH-sensing coating.

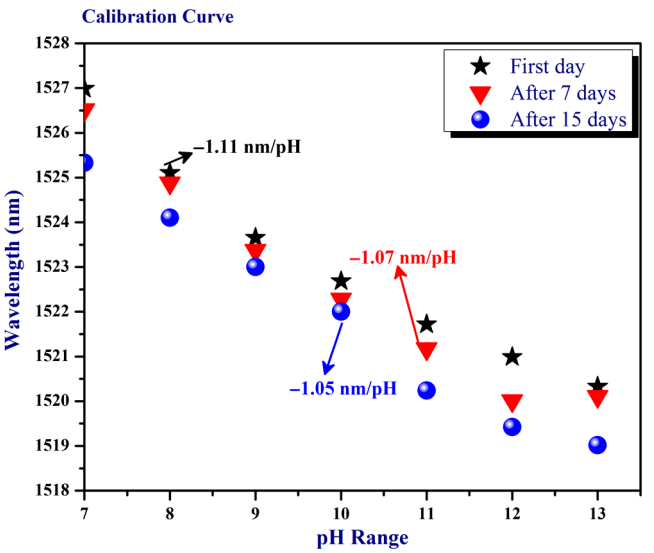

Fig. 10 Calibration curve for pH sensor.

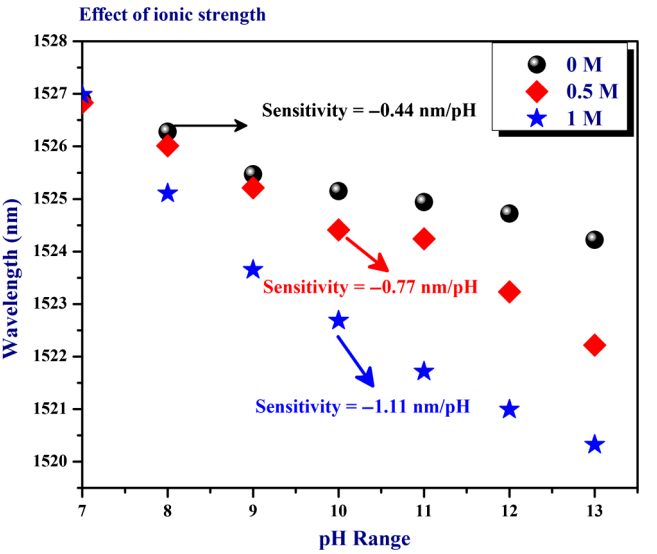

Fig. 11 Variation of wavelength as a function of pH range with ionic strength with different molar concentration.

6.3 *Impact of Temperature*

First, the experiment was performed to investigate the environmental effect on the sensor. The external environmental temperature effect on the fabricated probe was carried out by immersion of the fiber probe into a water bath with increasing temperatures from 25°C to 38°C. The shifts in wavelength with temperature are depicted in Fig. 12, and the temperature sensitivity was found to be 0.0018 nm°C^{-1}, which is very small. The wavelength shift due to the increasing temperature is due to the fact that the temperature variation affects the hydrogel swelling coating and refractive index.

We have also investigated the effect of temperature on the reflection spectrum of the pH sensor. The result indicates that the device was not suitable for high temperatures. The experiment was performed for four different temperatures, 25°C, 30°C, 35°C, and 40°C, and the results evaluated for temperature response are plotted in Fig. 13.

The higher temperature affects the pH-sensing coat in various manners such as leaching of the dyes is increased or the thermal

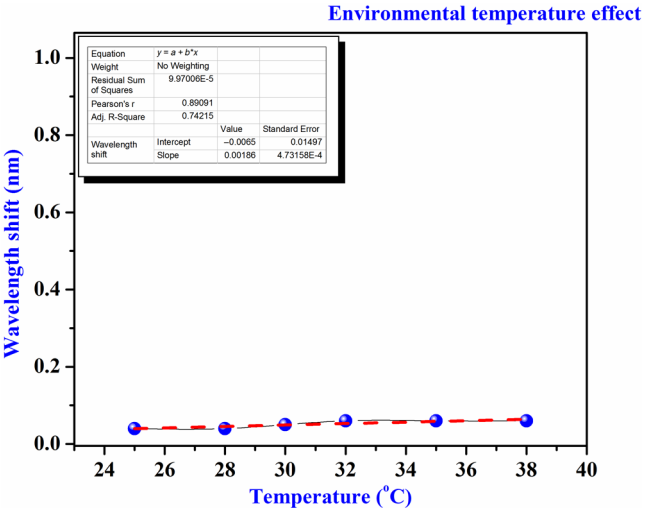

Fig. 12 Effect of environmental temperature on pH sensor.

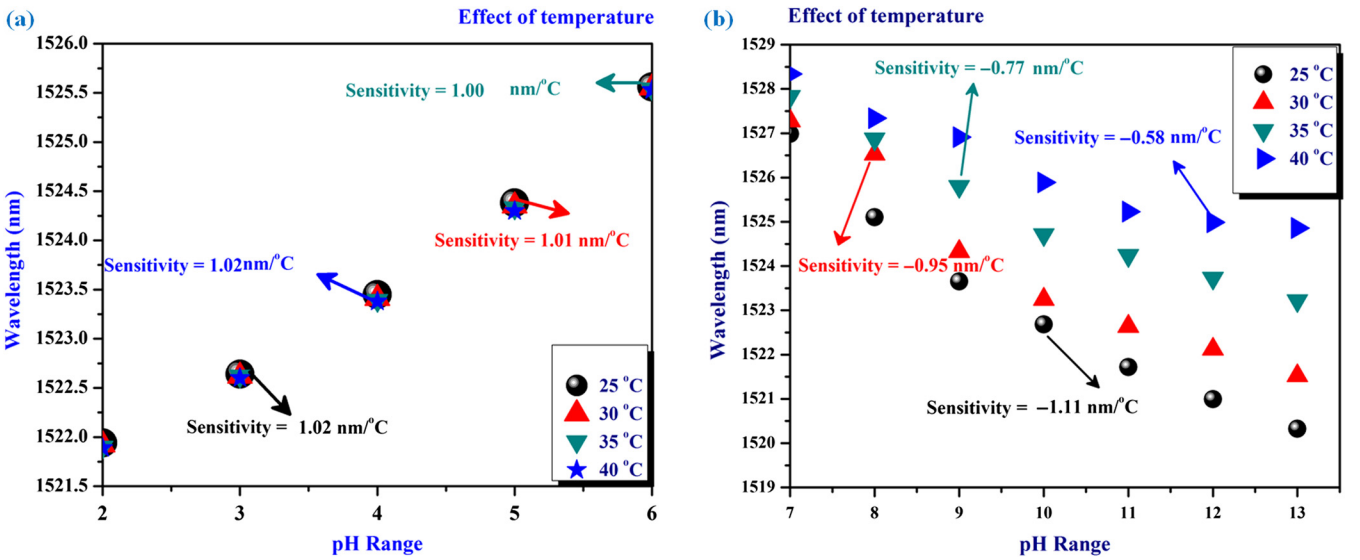

Fig. 13 Variation of wavelength with pH range for different temperatures of liquid.

expansion structure may be affected. The increasing or decreasing temperature may also affect the dissociation constant of indicators. The fabricated device revealed a negative behavior with temperature response because thermal expansion of pH-sensitive coating increases its volume and decreases RI. This leads to a blueshift of the wavelength dip. Therefore, the device is not suitable for high temperatures because a high temperature of the solution increases the ionization of H^+ and results in a decrement of the pH value. The increasing temperature affects both the acidic and alkaline solutions because of the activation of hydrogen ion. However, there is lesser variation in acidic solutions as compared to alkaline solutions. The pH-sensitive dyes have different behaviors for acidic and alkaline environments, and each form has different absorption spectra analyzed by Ref. 26. Thus, the increasing pH value of solutions with temperature helps to decrease the absorbance in cases of acidic solutions and increase it for alkaline solutions. In addition, the swelling of the hydrogel coating is more for alkaline solutions as compared with acidic.

7 Conclusions

In summary, a compact reflective optical fiber pH sensor has been proposed and experimentally demonstrated using SMF and NCF. After depositing sol–gel thin film on a surface of NCF by the dip-coating technique, the fabricated device has been used to measure pH of both acid and alkaline solutions. The sensitivity of the device was found to be 1.02 and −0.93 nm/pH for acid and alkaline solutions, respectively. The effect of ionic strength, temperature, and stability of device was also studied. The sensing over a wide pH range (2 to 13 pH) and the RI measurement with this kind of structure make our sensor unique in addition to its advantages, namely, compact size, ease of fabrication, high sensitivity, and good repeatability. Also, our present work overcomes the issues related to accurate pH measurement under the circumstances of extreme ionic concentrations.

Disclosures

The authors have no relevant financial interests in the paper and no other potential conflicts of interest.

Acknowledgments

This work was supported by IIT(ISM) Dhanbad, India, for financial support and Electrical and Engineering and Physics Department of IIT Madras for research facilities. The authors are also very thankful to Mr. Tejaswi Hegade, junior research fellow at VIT University, Chennai, for the valuable discussion.

References

1. A. Khorsandi et al., "Second-harmonic laser-coupled optical fiber sensor for pH measurement and corrosion detection based on evanescent field absorption," *Opt. Laser Technol.* **44**, 1564–1569 (2012).
2. X. Zhang, "New fluorescent pH probes for acid conditions," *Sens. Actuators B Chem.* **206**, 663–670 (2015).
3. A. K. Pathak et al., "Fabrication and characterization of TiO_2 coated cone shaped nano-fiber pH sensor," *Opt. Commun.* **386**, 43–48 (2017).
4. I. Kasik et al., "In vivo optical detection of pH in microscopic tissue samples of Arabidopsis thaliana," *Mater. Sci. Eng. C* **33**, 4809–4815 (2013).
5. S. A. Grant et al., "In vitro and in vivo measurements of fiber optic and electrochemical sensors to monitor brain tissue pH," *Sens. Actuators B Chem.* **72**, 174–179 (2001).
6. J. L. Peterson et al., "Fiber optic pH probe for physiological use," *Anal. Chem.* **52**, 864–869 (1980).
7. P. Ondrej et al., "Tapered optical fiber sensor for detection of pH in microscopic volumes," *Sens. Transducers* **27**, 312–318 (2014).
8. L. F. Rickelt et al., "Etching of multimode optical glass fibers: a new method for shaping the measuring tip and immobilization of indicator dyes in recessed fiber-optic microprobes," *Sens. Actuators B Chem.* **211**, 462–468 (2015).
9. B. D. Gupta and N. K. Sharma, "Fabrication and characterization of U-shaped fiber-optic pH probes," *Sens. Actuators B* **82**, 89–93 (2002).
10. A. Armin et al., "On the pH and concentration response of an evanescent field absorption sensor using a coiled-shape plastic optical fiber," *Sens. Actuators A* **165**, 181–184 (2011).
11. G. Beltran-Perez et al., "Fabrication and characterization of an optical fiber pH sensor using sol-gel deposited TiO_2 film doped with organic dyes," *Sens. Actuators B* **120**, 74–78 (2006).
12. S. Khodadoust et al., "Design of an optically stable pH sensor based on immobilization of Giemsa on triacetylcellulose membrane," *Mater. Sci. Eng. C* **57**, 304–308 (2015).
13. L. F. Rickelt et al., "Etching of multimode optical glass fibers: a new method for shaping the measuring tip and immobilization of indicator dyes in recessed fiber-optic microprobes," *Sens. Actuators B* **211**, 462–468 (2015).

14. G. Beltran-Perez et al., "Fabrication and characterization of an optical fiber pH sensor using sol-gel deposited TiO_2 film doped with organic dyes," *Sens. Actuators B* **120**, 74–78 (2006).
15. J. Rayss et al., "Optical aspects of Na+ ions adsorption on sol-gel porous films used in optical fiber sensors," *J. Colloid Interface Sci.* **250**, 168–174 (2002).
16. M. V. Foguel et al., "A molecularly imprinted polymer-based evanescent wave fiber optic sensor for the detection of basic red 9 dyes," *Sens. Actuators B* **218**, 222–228 (2015).
17. V. Bhardwaj and V. K. Sigh, "Study of liquid sealed no-core fiber interferometer for sensing applications," *Sens. Actuator A Phys.* **254**, 95–100 (2017).
18. V. Bhardwaj et al., "Silicone rubber coated highly sensitive optical fiber sensor for temperature measurement," *Opt. Eng.* **55**(12), 126107 (2016).
19. X. Liu et al., "Multi-point fiber-optic refractive index sensor by using coreless fibers," *Opt. Commun.* **365**, 168–172 (2016).
20. V. Bhardwaj et al., "Experimental and theoretical analysis of connector offset optical fiber refractive index sensor," *Plasmonics* 1–6 (2016).
21. Y. Zhao et al., "Refractive index sensing based on photonic crystal fiber interferometer structure with up-tapered joints," *Sens. Actuators B* **221**, 406–410 (2015).
22. Y. Zhao et al., "A highly sensitive Mach–Zehnder interferometric refractive index sensor based on core-offset single mode fiber," *Sens. Actuator A* **223**, 119–124 (2015).
23. C. R. Zamarreño et al., "Optical fiber pH sensor based on lossy-mode resonances by means of thin polymeric coatings," *Sens. Actuators B* **155**, 290–297 (2011).
24. J. Goicoechea et al., "Utilization of white light interferometry in pH sensing applications by mean of the fabrication of nanostructured cavities," *Sens. Actuators B* **138**, 613–618 (2009).
25. P. Hu et al., "Photonic crystal fiber interferometric pH sensor based on polyvinyl alcohol/polycrylic acid hydrogel coating," *Appl. Opt.* **54**, 2647–2652 (2015).
26. W. S. Tan et al., "Temperature-induced, reversible swelling transitions in multilayers of a cationic triblock copolymer and a polyacid," *Macromolecules* **43**, 1950–1957 (2010).

Vanita Bhardwaj received her MSc degree in physics from GVM Girls College, Sonepat and Haryana, India. Currently, she is working as a senior research fellow in the Department of Applied Physics, IIT (ISM, Dhanbad) under the guidance of Dr. Vinod K. Singh. Her area of research interests include design and characterize fiber optic sensor.

Akhilesh Kumar Pathak received his MSc degree from University of Allahabad in 2012. Currently, he is working as a senior research fellow in the Indian Institute of Technology (Indian School of Mines), Dhanbad, under the supervision of Dr. V.K. Singh. His area of research interests include design and fabricate optical fiber-based sensors and their application in pH and biomedical sensing.

Vinod Kumar Singh did his MSc degree in physics from Bhagalpur University, Bihar. He has completed his MPhil and PhD degrees from IIT (ISM), Dhanbad, Jharkhand, India. Currently, he is an associate professor in the Department of Applied Physics, IIT (ISM, Dhanbad). His area of research interests include fiber optic sensor and design, fabrication and characterization of PCFs. He has published more than 70 papers so far in different journals and conferences.